Published in final edited form as:
Biochemistry. 2013 December 23; 52(51): 9358–9366. doi:10.1021/bi4010446.

The Structure of MurNAc 6-Phosphate Hydrolase (MurQ) from *Haemophilus influenzae* with Bound Inhibitor

Timin Hadi[†,‡], **Saugata Hazra**[†,‡], **Martin E. Tanner**[§,*], and **John S. Blanchard**[†,*]

[†]Department of Biochemistry, Albert Einstein College of Medicine, 1300 Morris Park Avenue, Bronx, New York, USA 10461

[§]Department of Chemistry, University of British Columbia, Vancouver, British Columbia, Canada V6T 1Z1

Abstract

The breakdown and recycling of peptidoglycan, an essential polymeric cell structure, occurs in a number of bacterial species. A key enzyme in the recycling pathway of one of the components of the peptidoglycan layer, *N*-acetylmuramic acid (MurNAc), is MurNAc 6-phosphate hydrolase (MurQ). This enzyme catalyzes the cofactor-independent cleavage of a relatively non-labile ether bond and presents an interesting target for mechanistic studies. Open-chain product and substrate analogs were synthesized and tested as competitive inhibitors (K_{is} values of 1.1 +/− 0.3 mM and 0.23 +/− 0.02 mM, respectively) of the MurNAc 6P hydrolase from *Escherichia coli* (MurQ-EC). To identify the roles of active site residues important for catalysis, the substrate analog was co-crystallized with the MurNAc 6P hydrolase from *Haemophilus influenzae* (MurQ-HI) that was amenable to crystallographic studies. The co-crystal structure of MurQ-HI with the substrate analog showed that Glu89 was located in close proximity to both the carbon at the C2 position and the oxygen at the C3 position of the bound inhibitor, and that no other potential acid/base residue that could act as an active site acid/base was located in the vicinity. The conserved residues Glu120 and Lys239 were found within hydrogen-bonding distance of the C5 hydroxyl group and C6 phosphate group, suggesting that they play a role in substrate binding and ring-opening. Combining these results with previous biochemical data, a one base mechanism of action where Glu89 functions to both deprotonate at the C2 position and assist in the departure of the lactyl ether at the C3 position is proposed. This same residue would serve to deprotonate the incoming water and reprotonate the enolate in the second half of the catalytic cycle.

Keywords

MurQ; YfeU; MurNAc 6P hydrolase; etherase; peptidoglycan; recycling

Peptidoglycan is an essential portion of the bacterial cell wall in both Gram-positive and Gram-negative bacteria.[(1)] This polymeric structure functions as a physical barrier from the environment and is important in preventing lysis due to the large osmotic pressure exerted upon the cell. The structure of peptidoglycan is comprised of alternating *N*-

[*]To whom correspondence should be addressed: Department of Biochemistry, Albert Einstein College of Medicine, 1300 Morris Park Ave., Bronx, NY, USA 10461. Phone: (718) 430-3096. Fax: (718) 430-8565. john.blanchard@einstein.yu.edu; Department of Chemistry, University of British Columbia, Vancouver, British Columbia, Canada V6T 1Z1. Phone: (604) 822-9453. Fax: (604) 822-2847. mtanner@chem.ubc.ca.
[‡]These authors contributed equally.

Supporting Information. ^{1}H NMR spectra of compounds **1** and **2**, inhibitor kinetic data with MurQ-EC, multiple sequence alignment, and crystallographic data tables can be found in the supporting information. This material is available free of charge via the Internet at http://pubs.acs.org.

acetylglucosamine (GlcNAc) and *N*-acetylmuramic acid (MurNAc) monosaccharides linked together via β-(1→4) glycosidic linkages. Amino acids are attached to the D-lactyl ether moiety at the C3 position of the MurNAc residues and it is through these amino acids that cross-links are formed between neighboring strands to create the three dimensional structure that surrounds the bacterial cell. Although the exact composition of the peptidoglycan layer can vary immensely from organism to organism, or under different physiological conditions, for the most part the repeating disaccharide unit remains the same.[1, 2]

Because of its essential nature and the key role that it plays during the bacterial cell life cycle, significant research effort has focused on understanding the biosynthesis and metabolism of peptidoglycan. The metabolism of peptidoglycan via recycling and salvage pathways has been studied in a number of organisms, but perhaps most extensively in the Gram-negative bacterium *Escherichia coli*.[3] A number of more recent studies have examined the fate of the monosaccharide MurNAc in the peptidoglycan recycling pathway in *E. coli*.[4–7] Briefly, the disaccharide unit is first cleaved by the glycosidase NagZ to generate GlcNAc and 1,6-anhydro-*N*-acetylmuramic acid; the anhydro sugar is then converted by the hydrolyzing-kinase, AnmK, to generate *N*-acetylmuramic acid 6-phosphate (MurNAc 6P); finally, the D-lactyl ether of MurNAc 6P is cleaved by the MurNAc 6P hydrolase, MurQ, to generate *N*-acetylglucosamine 6-phosphate (GlcNAc 6P), for assimilation in the GlcNAc recycling pathway (Figure 1).

The MurQ hydrolase is a particularly interesting target for mechanistic studies as it catalyzes the cleavage of a non-labile ether bond at the C3 position of MurNAc 6P. Previous work has provided a proposed mechanism of action and helped to identify possible active site residues involved in catalysis (Figure 2).[6, 7] A ring-opening of MurNAc 6P, likely enzyme-catalyzed, first serves to generate the C1 aldehyde and consequently acidifies the hydrogen at the C2 position. This hydrogen is deprotonated by an active site acid/base residue (B_1) to generate a resonance-stabilized enolate anion. The enolate then undergoes a *syn*-elimination of D-lactate, aided by a catalytic acid/base residue (B2), to generate a Δ2,3-unsaturated (*E*)-alkene intermediate.[7] In a sequence that mirrors the elimination of lactate, B_2 first serves to deprotonate an incoming water molecule for addition at the C3 position of the alkene intermediate to generate the enolate anion. This enolate is then protonated at the C2 position by B_1 to generate the open chain form of GlcNAc 6P. Ring closure then generates the two anomers of the pyranose form of GlcNAc 6P. Experiments using site-directed mutants identified Glu83 and Glu114 as key residues for catalysis, and tentatively assigned their roles as B_2 and B_1, respectively, in the proposed mechanism.[7]

MurQ has not been deemed essential in *E. coli*, but there is a dearth of information regarding the enzyme's role in peptidoglycan recycling in other microorganisms.[8, 9] Interestingly, recent studies have indicated that homologs in other organisms play a more important role under certain growth conditions.[10] With these considerations in mind, the synthesis and testing of compounds **1** and **2** as potential inhibitors of MurQ from *E. coli* (referred to as MurQ-EC for clarity) was undertaken (Figure 2). Compounds **1** and **2** are analogs of GlcNAc 6P and MurNAc 6P that are reduced at the C1 position. They were designed to mimic the open chain forms of the product and substrate while lacking the acidic hydrogen at the C2 position that is necessary for MurQ catalysis to occur. These compounds could also serve as useful tools for probing the active site acid/base residues important for MurQ catalysis in a co-crystal structure. Although the crystal structure of the *E. coli* enzyme has yet to be solved, a crystal structure of a homolog of MurQ from *Haemophilus influenzae* was previously reported as a part of structural genomics project (previously referred to as YfeU but has been re-assigned as MurQ and will be referred to as MurQ-HI in this manuscript).[11] In this study, the co-crystal structure of the enzyme MurQ-HI from *H. influenzae* with compound **2** is reported (PDB ID code: 4LZJ). The activity of the *H.*

influenzae MurQ homolog as a MurNAc 6P hydrolase was confirmed, and analysis of the active site acid/base residues surrounding the bound compound **2** was performed. The new information garnered from this structure is used along with previous mechanistic studies to propose a modified mechanism of enzyme action.

EXPERIMENTAL PROCEDURES

Materials and General Methods

MurNAc 6P was prepared in six chemical steps from GlcNAc as described previously.[7] ^{1}H NMR spectra were acquired on a Bruker DRX300 instrument at a field strength of 300 MHz. Mass spectrometry was performed by electrospray ionization (ESI-MS) using an Esquire LC mass spectrometer in negative mode. Protein concentrations were determined by Bradford analysis using bovine serum albumin as the standard.

Reduced GlcNAc 6P Inhibitor (1)

GlcNAc 6P (56 mg, 0.173 mmol) was dissolved in D_2O and sodium borohydride was added (50 mg, 1.32 mmol). The mixture was then transferred to a NMR tube and heated at 37 °C overnight. The ^{1}H NMR spectrum of the mixture taken after overnight incubation revealed that the peaks corresponding to the anomeric hydrogens of GlcNAc 6P were absent, suggesting that the reduction of the aldehyde at the C1 position was complete. The pH of the reaction was adjusted to 2.0 by the addition of acetic acid, and concentrated *in vacuo*. Toluene was added to the residue and the mixture was concentrated *in vacuo* to remove residual acetic acid. The crude product was dissolved in H_2O and applied to a 5 mL column of AG-1X8 resin (formate form); the resin was then washed successively with 50 mL H_2O, 50 mL 1.4 N formic acid, 50 mL 2.8 N formic acid, and finally 100 mL of 5.6 N formic acid. Each fraction was analyzed by mass spectrometry and those containing compound **1** were pooled and their volume was reduced *in vacuo*. Distilled water was added to the solution and the remaining solvent was evaporated; this procedure was repeated multiple times to remove residual formic acid. Compound **1** (37 mg, 0.122 mmol, 70%) was dissolved in H_2O and the pH of the solution was adjusted to 7.1 with 0.1 N NaOH. The solution was frozen and lyophilized to give the sodium salt of 1 as a white powder. ^{1}H NMR (Figure S1, 300 MHz, D_2O) δ 4.05 – 3.80 (m, 4H), 3.76 – 3.37 (m, 4H), 1.95 (s, 3H). ESI-MS *m/z* 302.1 $[M - H]^-$.

Reduced MurNAc 6P Inhibitor (2)

MurNAc 6P (29 mg, 0.069 mmol) was dissolved in 100 mM deuterated triethanolamine buffer (pD 8.0) and sodium borohydride (53 mg, 1.40 mmol) was added. The solution was stirred at room temperature for 48 h and a portion was transferred to a NMR tube for analysis by ^{1}H NMR spectroscopy. The ^{1}H NMR spectrum of the solution revealed that the peaks corresponding to the anomeric hydrogens of MurNAc 6P were absent, suggesting that the reduction of the aldehyde at the C1 position was complete. The reaction was frozen and subsequently lyophilized to give a white powder. The crude product was dissolved in H_2O and applied to a 5 mL column of AG-1X8 resin (formate form); the resin was then washed successively with 100 mL H_2O, 50 mL 1.4 N formic acid, 100 mL 2.8 N formic acid, and finally 100 mL of 5.6 N formic acid. Each fraction was analyzed by mass spectrometry and those containing compound **2** were pooled and their volume was reduced *in vacuo*. Distilled water was added to the solution and the remaining solvent was evaporated; this procedure was repeated multiple times to remove residual formic acid. Compound **2** (23 mg, 0.060 mmol, 88%) was dissolved in H_2O and the pH of the solution was adjusted to 8.3 with 0.1 N NaOH. The solution was frozen and lyophilized to give the sodium salt of compound **2** as a white powder. ^{1}H NMR (Figure S2, 300 MHz, D_2O) δ 4.11 – 3.95 (m, 2H), 3.91 – 3.78 (m,

3H), 3.74 – 3.48 (m, 4H), 1.94 (s, 3H), 1.27 (d, J = 6.8 Hz, 3H). ESI-MS m/z 374.1 [M – H]$^-$.

Cloning, Overexpression and Purification of E. coli MurQ (MurQ-EC) and H. influenzae MurQ (MurQ-HI)

Wild-type MurQ-EC enzyme from *E. coli* was overexpressed and purified as described previously.[6, 7] Enzyme used for kinetic studies was prepared fresh from frozen cell pellets as required due to its reported instability.

The *H. influenzae* MurQ-HI gene (HI0754) was PCR amplified from *H. influenzae* KW20 Rd genomic DNA as a template using 5′– GGT ATT GAG GGT CGC ATG AAT GAC ATT ATA TTA AA –3′ as the forward primer and 5′ – AGA GGA GAG TTA GAG CCT TAT TTA GAA AGC GCA TTT C – 3′ as the reverse primer. The underlined sequences are the overhang regions designed for ligation-independent cloning. The PCR product was cloned into the pET-30 Xa/LIC vector (Novagen) according to the manufacturer's protocol. The recombinant plasmid, encoding for the MurQ-HI gene product with a N-terminal hexa-histidine tag and a Factor Xa cleavage site, was amplified using NovaBlue GigaSingles competent cells (Novagen) and the MurQ-HI gene sequence was subsequently verified.

The recombinant MurQ-HI-containing pET-30 Xa/LIC plasmid was transformed into T7 Express *E. coli* competent cells and plated on LB Agar plates containing (30 μg/mL) kanamycin. The transformed *E. coli* cells were grown overnight at 37 °C while shaking at 225 rpm in 30 mL of LB medium containing 30 μg/mL kanamycin. This starter culture was used to inoculate 6 L of LB medium containing 30 μg/mL kanamycin and the resultant mixture was incubated at 37 °C while shaking at 225 rpm until an A_{600} of 0.6 was reached. Isopropyl β-D-galactopyranoside (IPTG) was added to a final concentration of 0.5 mM and the cultures were grown for an additional 3.5 h at 37 °C. The cells were harvested by centrifugation at 4,000 rpm for 15 minutes and the cell pellet was stored at −78 °C. The pelleted cells were resuspended in 70 mL of phosphate buffer (50 mM, 500 mM NaCl, 10 mM imidazole, pH 8.0) containing one tablet of Complete EDTA-free proteases inhibitor cocktail, and lysed by multiple passages through a cell homogenizer (15,000 psi). The lysate was centrifuged at 15,000 rpm for 40 min and then poured into 5 mL of Ni-NTA agarose resin. The lysate-resin mixture was mixed for 20 min at 4 °C before being poured into a disposable column. The resin was washed with phosphate buffer (50 mM, 500 mM NaCl, pH 8.0) containing increasing amounts of imidazole (10 mM, 50 mM, 500 mM) in a stepwise fashion. Fractions were analyzed by SDS-PAGE and those containing the MurQ-HI protein were pooled and dialyzed overnight at 4 °C against 4 L of Tris buffer (50 mM, 300 mM NaCl, pH 7.5). The protein was concentrated using an Amicon 10K MWCO centrifugal device and loaded onto a Hiload 26/60 Superdex 200 preparatory grade gel filtration column. The column was washed with Tris buffer (50 mM, 300 mM NaCl, pH 7.5) and MurQ-HI-containing fractions were pooled and concentrated using an Amicon 10K MWCO centrifugal device. Glycerol was added to the enzyme as a cryo-protectant (20% v/v) and the solution was stored at −78 °C.

For crystallographic studies, the N-terminal hexa-histidine tag was cleaved using Factor Xa (Novagen) according to the manufacturer's instructions. The cleavage of the protein was monitored by taking aliquots of the cleavage reaction at different time points and analyzing them by SDS-PAGE. The cleaved protein was exchanged into Tris buffer (50 mM, 300 mM NaCl, pH 7.5) and glycerol (20% v/v) was added. The MurQ-HI solutions (25 mg/mL) were snap frozen and stored at −78 °C until required for crystallization experiments.

Inhibitor Kinetics Assays

The inhibitory activity of compounds **1** and **2** on the enzymatic activity of MurQ-EC was determined using a coupled spectrophotometric assay monitoring the release of D-lactate as described previously.[7] All kinetic assays were performed at 30 °C in 60 mM triethanolamine-HCl buffer (pH 8.0) containing 0.65 mM *p*-iodonitrotetrazolium violet (INT), 5 mM NAD^+, 10 units of diaphorase, 30 units of D-lactate dehydrogenase, a fixed amount of MurQ-EC, and variable concentrations of MurNAc 6P and either compound **1** or **2** (total volume of 1 mL). MurQ-EC dilutions for kinetic assays were stabilized by the addition of 5% (v/v) of a 10 mg/mL BSA solution in H_2O. Each assay was initiated by the addition of MurNAc 6P after incubation at 30 °C for 10 min. The rate was determined by measuring the change in absorbance at 500 nm due to the reduction of INT. Initial rates were fit to equation 1 for competitive inhibition using Sigmaplot, version 11.0, and the kinetic parameters were determined using this fit.

$$v = k_{\mathrm{cat}}{}^{*}[\mathrm{S}]/K_{\mathrm{s}}{}^{*}(1+[\mathrm{I}]/K_{\mathrm{is}})+[\mathrm{S}] \quad (1)$$

Crystallography

Protein crystallization was performed by using the sitting drop vapor diffusion method. The initial MurQ-HI protein sample (8 mg/ml, 200 mM NaCl, 50 mM HEPES and 5% glycerol) was screened using MCSG crystal screens I-IV. Flat thin crystals were obtained using condition MCSGI-B2 (0.2 M NaCl, 0.1 M Bis-Tris:HCl, pH 5.5, 25% (w/v) PEG 3350) and thin needle type crystals appeared from condition MCSGIII-G6 (0.17 M ammonium sulfate, 25.5% (w/v) PEG 4000, 15% (v/v) glycerol). Iterated micro-seeding resulted in efficient crystal growth as well as improved morphology, producing diffraction quality crystals of the protein. Significant improvement was observed for the crystals obtained from the MCSGI-B2 condition and these were used for future experiments. The crystals were incubated at room temperature (298K).

Soaking, Data Collection & Refinement

Crystals of the refined apo proteins appeared after 5 days. Before data collection, the crystals were flash-frozen in liquid N_2 using mineral oil as a cryo-protectant. Diffraction data was collected from a single frozen crystal using a RAXIS-IV^{++} detector mount on a Rigaku RH-200 rotating anode (copper anode) x-ray generator. The data were processed using HKL2000.[12] A previously solved structure of MurQ-HI (previously called YfeU, PDB entry 1NRI)[11] was used to phase the data using the CCP4 software suite.[13] Multiple rounds of structural refinement and model building were performed in Refmac5, Phenix[14–16] and Coot.[17] Structure figures were generated using PyMOL.[18] Atomic coordinates and experimental structure factors have been deposited in the Protein Data Bank (PDB ID code: 4M0D). The crystals belong to $P2_12_12_1$ space group with cell dimensions a = 76.13 Å, b = 111.65 Å, c = 134.51 Å, $\alpha = \beta = \gamma = 90.00$ degrees. Table S1 (Supporting Information) lists the other data collection statistics as well as the final refinement statistics for the apo structure.

Diffraction quality MurQ-HI apo crystals were soaked with 50 mM of compound **2** in mother liquor. Crystals were flash frozen after soaking of 60, 120 & 180 minutes respectively. Before freezing, mineral oil was added to the solution as a cryo-protectant. Diffraction data was collected from a single crystal soaked for 120 minutes.

Data collection and refinement were performed using the same methods described above. Atomic coordinates and experimental structure factors have been deposited in the Protein

Data Bank (PDB ID code: 4LZJ). Table S2 (Supporting Information) lists the data collection statistics as well as the final refinement statistics for structure of the MurQ-HI-Compound **2** complex.

RESULTS

Testing of compounds 1 and 2 as inhibitors of MurQ-EC

Open-chain analogs of the product and substrate were expected to serve as inhibitors of the MurQ-catalyzed reaction. Compounds **1** and **2** were synthesized through borohydride reduction of GlcNAc 6P and MurNAc 6P, respectively, and tested as inhibitors of *E. coli* MurQ activity. Both compounds acted as competitive inhibitors of MurQ-EC with K_{is} values of 1.1 +/− 0.3 mM (Figure S3) and 0.23 +/− 0.02 mM (Figure S4), respectively.

Crystallographic studies on MurQ-HI

The MurQ-HI protein containing a N-terminal hexahistidine tag was overexpressed in *E. coli* and purified. The recombinant protein was incubated with MurNAc 6P and shown to be active as a MurNAc 6P hydrolase (data not shown). Crystals of MurQ-HI were grown and the apo enzyme structure was solved to a resolution of 2.6 Å. Crystals of the apo enzyme were then soaked with compound **2** in order to obtain an enzyme-inhibitor complex. The complex containing compound **2** was solved to a resolution of 2.4 Å. The structures of the apo enzyme and the enzyme in complex with compound **2** were solved as tetramers by molecular replacement using 1NRI as the template.[11]

The MurQ-HI tetramer is composed of four monomers (labeled A through D, Figure 3A) and each of these monomers is composed of two domains, labeled I and II (Figure 3B). The N-terminal domain I is the larger and more rigid domain and is comprised of six alpha helices and five beta sheets. The five beta sheets are surrounded by alpha helices on both the concave and convex sides. Domain II is comprised of five alpha helices and is linked to domain I by a long flexible linker (Figure 3B). A portion of domain II was absent in the previously solved apo structure of MurQ-HI; in this study, we present the full length structure of the protein, including this previously unsolved region of domain II (Figure 3C). The overall structure of the monomer is an α/β/α sandwich that is analogous to the NAD(P)/FAD-binding Rossmann fold. This domain fold is commonly found in many proteins related to phosphosugar-like isomerases, phosphosugar binding proteins, and regulatory proteins controlling the expression of genes involved in the synthesis of phosphosugars.[19–21]

In both of the solved structures, two dimers are formed, one between monomers A–D and the other between B–C (Figure 4A). The dimers are formed by the head-to-tail interactions between each of the monomers. Five secondary structural constituents play an important role in forming the dimer interface; the interacting components on each monomer are helices α1, α2, α6 and both the N-terminal and domain connector loop (Figure 4B). The active site is constructed by the contribution of two separate monomers from each of the dimer pairs (A–D, B–C). In the case of the A–D dimer in complex with compound **2**, the active site is formed by Thr93, Gln89 and Lys239 from monomer A, while Thr78, Ser79, Arg81, Glu120, Ala146, Ser147 and Thr150 residues are contributed by monomer D (Figure 5). Additional electron density due to compound **2** is present in the active site (Figure 5, inset) and a number of active site residues are found in close proximity to the inhibitor. The carboxylic acid oxygen of the putative acid/base catalyst Glu89 (monomer A, Glu83 in MurQ-EC) is located 3.2 Å away from the C3 oxygen and 3.3 Å away from C2 of compound **2**. Glu120 (monomer D, Glu114 in MurQ-EC) is located 2.8 Å away from the C5 oxygen but not in close proximity to either the carbon at C2 (6.6 Å) or the C3 oxygen (5.1 Å) of compound **2**.

The Lys239 (monomer A) ε-amino group is located 2.5 Å away from the C5 oxygen, 2.9 Å away from the C6 oxygen and 3.8 Å away from the C6 phosphate oxygen.

DISCUSSION

The results of the inhibitor design and crystallographic studies reported in this manuscript provide additional insight into the proposed mechanism of action of MurNAc 6P hydrolases outlined in Figure 2. When combined with previous biochemical studies on this class of enzymes,[7] the crystallographic data obtained with bound inhibitors allows for a more definitive assignment of specific roles to important active site acid/base residues involved in catalysis. The synthesis of compounds **1** and **2** represents the first reported attempts at inhibitor design for the MurNAc 6P hydrolase enzyme. These compounds are analogs of the open-chain sugars formed as intermediates in the MurQ reaction. They may therefore be expected to bind with greater affinity than the corresponding substrates. It has previously been established that Schiff's base formation is not involved in the MurQ reaction, and therefore reduction of the C1 aldehyde should not dramatically affect binding.[7] Compound **1**, a mimic of the open-chain GlcNAc 6P product of the reaction, does not function as a potent inhibitor of MurQ-EC with a K_{is} of 1.1 +/− 0.3 mM that is in the same range as the K_M of the MurNAc 6P substrate (1.2 +/− 0.1 mM). However compound **2**, a mimic of the MurNAc 6P substrate of the reaction, is a 5-fold better inhibitor of MurQ-EC with a K_{is} of 0.23 +/− 0.02 mM. That the substrate analog of this reaction is a more potent inhibitor than the product analog is not unexpected, and we hypothesize that this is due to the additional binding interactions gained by the presence of the D-lactyl ether group at the C3 position of compound **2**.

Neither of the compounds **1** and **2** underwent any reaction in the presence of MurQ-EC or MurQ-HI, providing further evidence that a carbonyl is required at the C1 position in order for catalysis to occur (Figure 2). This lack of reactivity with the enzyme allowed for the potential use of these compounds as active site probes in structural studies. The apo crystal structure of MurQ-HI from *H. influenzae* was previously reported as part of a structural genomics project (PDB code: 1NRI).[11] This protein was predicted to serve the same functional role as MurQ-EC from *E. coli* based on its high sequence identify (55%, E value 2e-95) and sequence similarity (72%). The coordinates of the MurQ-HI structure, along with those of the homologous enzyme glucosamine 6-phosphate synthase (GlmS), were previously used as the basis of a structural model of MurQ-EC.[7, 9] This model was used to successfully to identify the catalytically important active site residues Glu83 and Glu114.[7] These observations, along with the reported instability of MurQ-EC,[6] led us to believe that MurQ-HI would be a superior system for studying the structure of inhibitor complexes via X-ray crystallography.

The MurQ-HI complex with compound **2** represents the first crystal structure of a MurNAc 6P hydrolase with a bound inhibitor. A literature search revealed that outside of the previously solved apo structure no structural information is available for proteins sharing more than 35% sequence identity to this protein family. Analysis of the co-crystal structure of MurQ-HI with compound **2** allowed for the examination of key contacts in the active site pocket. A multiple sequence alignment of MurNAc 6P hydrolases revealed that the residues Glu89 and Glu120 in MurQ-HI were conserved and were equivalent to Glu83 and Glu114, respectively, in MurQ-EC (see Figure S5 for sequence alignment). Glu89 is located 3.2 Å away from the C3 oxygen atom and 3.3 Å away from the C2 carbon atom, placing it in a position to perform either the role of B_1 or B_2 (or both) in the catalytic mechanism.

Previous studies on the Glu83 and Glu114 residues in the MurQ-EC enzyme tentatively assigned them as the acid-base residues involved in both the elimination of the D-lactate and

subsequent hydration of the (*E*)-alkene intermediate (B_1 and B_2, Figure 2).[7] This assignment was attributed to the dramatic drop in catalytic activity observed upon mutation of either residue. A low rate of solvent-derived deuterium incorporation occurred into the C-2 position of unreacted MurNAc 6P when the Glu83Ala reaction was performed in D_2O. Such a deuterium incorporation into residual pools of starting material was not observed when similar incubations were performed with wild type enzyme or a Glu114Ala mutant.[7] The incorporation of deuterium suggested that a base (B_1) was still available to deprotonate at the C2 position of the substrate in the Glu83Ala mutant. The lack of deuterium incorporation into residual pools of starting material with the wild type enzyme (despite possessing an intact B_1 and B_2) was attributed to the rapid, and essentially irreversible elimination of D-lactate following enzyme-catalyzed deprotonation of MurNAc 6P; this elimination was shown to be over 10,000 fold slower in the Glu83Ala mutant.[7] These observations led to the suggestion that Glu83 may act as B_2 in the MurQ reaction mechanism, and in turn that Glu114 may play the role of B_1.

Examination of the crystal structure of MurQ-HI with compound **2** however, is somewhat at odds with these previous assignments. No residue other than Glu89 (corresponding to Glu83 in *E. coli* MurQ) is located within 5.5 Å of the C2 position of the inhibitor. The high structural similarity between compound **2** and the open chain intermediate strongly suggests that Glu89 plays the role of B_1 and acts to deprotonate the C-2 position during catalysis. This raises the question as to how deuterium exchange can occur with the Glu83Ala mutant of the *E. coli* enzyme. One explanation is that the residues that stabilize the enolate are still present in this mutant and therefore the acidity of the C-2 position is still reduced. It may be possible that a surreptitious base in the enzyme active site is able to take the place of Glu83 and catalyze a slow deprotonation at the C-2 position. One such possible base is the carboxylate of the lactate side chain that might swing over and transiently occupy the position that is left vacant by the removal of the Glu γ-carboxylate. In this position it could catalyze the proton transfers that would explain the observed solvent isotope incorporation with the mutant. This notion is consistent with the observation that the Glu83Gln MurQ-EC mutant also shows dramatically impaired catalytic activity yet does not incorporate solvent derived deuterium. In this case, the Gln side chain sterically impedes the motion of the lactate group (or other surreptitious base) and prevents it from playing such a role. Glu120 (Glu114 in MurQ-EC) was previously implicated as an important active site residue in catalysis and a possible candidate for deprotonation as B_1. Examination of the current structure however, shows that it is located 6.6 Å away from the C2 position and is unlikely to play a role in deprotonation/protonation at this position.

As an alternative to the two-base mechanism outlined in Figure 2, we propose that a single active site residue functions to both deprotonate at the C2 position to generate the resonance-stabilized enolate anion and to assist in the departure of the D-lactate group at the C3 position during catalysis (Figure 6). This same residue would serve to deprotonate the incoming water and reprotonate the enolate in the second half of the catalytic cycle. A candidate for this role is Glu89 (Glu83 in MurQ-EC) as it is located in close proximity to both the C2 and C3 positions of compound **2** in the co-crystal structure with MurQ-HI. We propose that Glu120, positioned within 2.8 Å of the C5 hydroxyl group, does not function as B_1 or B_2 but plays an important role in binding and stabilization of the ring-opened form of the monosaccharide species and possibly in the ring-opening and ring-closing of the substrate and product of the reaction. The conserved Lys239 residue appears to play a role in binding of the phosphate group at the C6 position or in the stabilization of the ring-opened form of the substrate through an interaction with the C5 hydroxyl group. There are also a number of side chain and backbone hydrogen-bonding interactions surrounding the C1 oxygen that could be important in the binding of the carbonyl at the C1 position or the

stabilization of the corresponding enolate anion intermediate formed during the course of the enzymatic reaction.

Although compound **2** was not a potent inhibitor of the MurQ-EC enzyme, it served as an excellent active site probe in these crystallographic studies. Analysis of the interactions between compound **2** and the residues in the active site enabled the proposal of a revised mechanism of enzyme action where Glu89 plays a dual role in catalysis, and helped to identify many binding interactions that could be useful for inhibitor design. However, future efforts towards synthesizing inhibitors for the MurNAc 6P hydrolases will be largely dependent upon the characterization of the role of peptidoglycan recycling in pathogens other than *E. coli*.

Supplementary Material

Refer to Web version on PubMed Central for supplementary material.

Acknowledgments

This work was supported by the National Institutes of Health Grant AI60899 to J.S.B. and a grant from the Natural Sciences and Engineering Council of Canada to M. E. T.

We would like to thank members of the laboratory of Dr. Steven Almo, particularly Yuriy Patskovsky, Rahul C. Bhosle and Matthew W. Vetting for aiding in crystallization efforts.

ABBREVIATIONS

anhMurNAc	1,6-anhydro-*N*-acetylmuramic acid
EDTA	ethylenediaminetetraacetic acid
ESI-MS	electrospray ionization mass spectrometry
FAD	flavin adenine dinucleotide
GlcNAc	*N*-acetylglucosamine
GlcNAc 6P	*N*-acetylglucosamine 6-phosphate
GlmS	*N*glucosamine 6-phosphate synthase
HEPES	4-(2-Hydroxyethyl)piperazine-1-ethanesulfonic acid
INT	*p*-iodonitrotetrazolium violet
IPTG	Isopropyl β-D-galactopyranoside
LB	Luria broth
MurNAc	*N*-acetylmuramic acid
MurNAc 6P	*N*-acetylmuramic acid 6-phosphate
MurQ	*N*-acetylmuramic acid 6-phosphate hydrolase
MWCO	molecular weight cutoff
NAD^+	nicotinamide adenine dinucleotide (oxidized form)
NADP	nicotinamide adenine dinucleotide phosphate
Ni-NTA	nickel nitriloacetic acid
PCR	polymerase chain reaction

PEG polyethylene glycol

References

1. Vollmer W, Blanot D, De Pedro MA. Peptidoglycan structure and architecture. FEMS Microbiol Rev. 2008; 32:149–167. [PubMed: 18194336]
2. Vollmer W. Structural variation in the glycan strands of bacterial peptidoglycan. FEMS Microbiol Rev. 2008; 32:287–306. [PubMed: 18070068]
3. Park JT, Uehara T. How bacteria consume their own exoskeletons (turnover and recycling of cell wall peptidoglycan). Microbiol Mol Biol Rev. 2008; 72:211. [PubMed: 18535144]
4. Dahl U, Jaeger T, Nguyen BT, Sattler JM, Mayer C. Identification of a phosphotransferase system of *Escherichia coli* required for growth on *N*-acetylmuramic acid. J Bacteriol. 2004; 186:2385–2392. [PubMed: 15060041]
5. Uehara T, Suefuji K, Valbuena N, Meehan B, Donegan M, Park JT. Recycling of the anhydro-*N*-acetylmuramic acid derived from cell wall murein involves a two-step conversion to *N*-acetylglucosamine-phosphate. J Bacteriol. 2005; 187:3643–3649. [PubMed: 15901686]
6. Jaeger T, Arsic M, Mayer C. Scission of the lactyl ether bond of *N*-acetylmuramic acid by *Escherichia coli* “etherase”. J Biol Chem. 2005; 280:30100–30106. [PubMed: 15983044]
7. Hadi T, Dahl U, Mayer C, Tanner ME. Mechanistic studies on *N*-acetylmuramic acid 6-phosphate hydrolase (MurQ): an etherase involved in peptidoglycan recycling. Biochemistry. 2008; 47:11547–11558. [PubMed: 18837509]
8. Reith J, Mayer C. Peptidoglycan turnover and recycling in Gram-positive bacteria. Appl Microbiol Biotechnol. 2011; 92:1–11. [PubMed: 21796380]
9. Jaeger T, Mayer C. *N*-acetylmuramic acid 6-phosphate lyases (MurNAc etherases): role in cell wall metabolism, distribution, structure, and mechanism. Cell Mol Life Sci. 2008; 65:928–939. [PubMed: 18049859]
10. Jiang H, Kong R, Xu X. The *N*-acetylmuramic acid 6-phosphate etherase gene promotes growth and cell differentiation of cyanobacteria under light-limiting conditions. J Bacteriol. 2010; 192:2239–2245. [PubMed: 20139182]
11. Kim Y, Quartey P, Ng R, Zarembinski TI, Joachimiak A. Crystal structure of YfeU protein from *Haemophilus influenzae*: a predicted etherase involved in peptidoglycan recycling. J Struct Funct Genomics. 2009; 10:151–156. [PubMed: 19234762]
12. Otwinowski Z, Minor W. Processing of X-ray diffraction data collected in oscillation mode. Methods Enzymol. 1997; 276:307–326.
13. Potterton E, Briggs P, Turkenburg M, Dodson E. A graphical user interface to the CCP4 program suite. Acta Crystallogr Sect D: Biol Crystallogr. 2003; 59:1131–1137. [PubMed: 12832755]
14. Adams PD, Afonine PV, Bunkoczi G, Chen VB, Davis IW, Echols N, Headd JJ, Hung LW, Kapral GJ, Grosse-Kunstleve RW, McCoy AJ, Moriarty NW, Oeffner R, Read RJ, Richardson DC, Richardson JS, Terwilliger TC, Zwart PH. PHENIX: a comprehensive Python-based system for macromolecular structure solution. Acta Crystallogr Sect D: Biol Crystallogr. 2010; 66:213–221. [PubMed: 20124702]
15. Murshudov GN, Vagin AA, Dodson EJ. Refinement of macromolecular structures by the maximum-likelihood method. Acta Crystallogr Sect D: Biol Crystallogr. 1997; 53:240–255. [PubMed: 15299926]
16. Pannu NS, Murshudov GN, Dodson EJ, Read RJ. Incorporation of prior phase information strengthens maximum-likelihood structure refinement. Acta Crystallogr Sect D: Biol Crystallogr. 1998; 54:1285–1294. [PubMed: 10089505]
17. Emsley P, Cowtan K. Coot: model-building tools for molecular graphics. Acta Crystallogr Sect D: Biol Crystallogr. 2004; 60:2126–2132. [PubMed: 15572765]
18. Schrodinger, L. The PyMOL Molecular Graphics System, Version 1.3r1. 2010.

19. Sorensen KI, Hove-Jensen B. Ribose catabolism of *Escherichia coli*: Characterization of the *rpiB* gene encoding ribose phosphate isomerase B and of the *rpiR* gene, which is involved in regulation of *rpiB* expression. J Bacteriol. 1996; 178:1003–1011. [PubMed: 8576032]

20. Peschke U, Schmidt H, Zhang HZ, Piepersberg W. Molecular characterization of the lincomycin-production gene cluster of *Streptomyces lincolnensis* 78-11. Mol Microbiol. 1995; 16:1137–1156. [PubMed: 8577249]

21. Teplyakov A, Obmolova G, Badet-Denisot MA, Badet B. The mechanism of sugar phosphate isomerization by glucosamine 6-phosphate synthase. Prot Sci. 1999; 8:596–602.

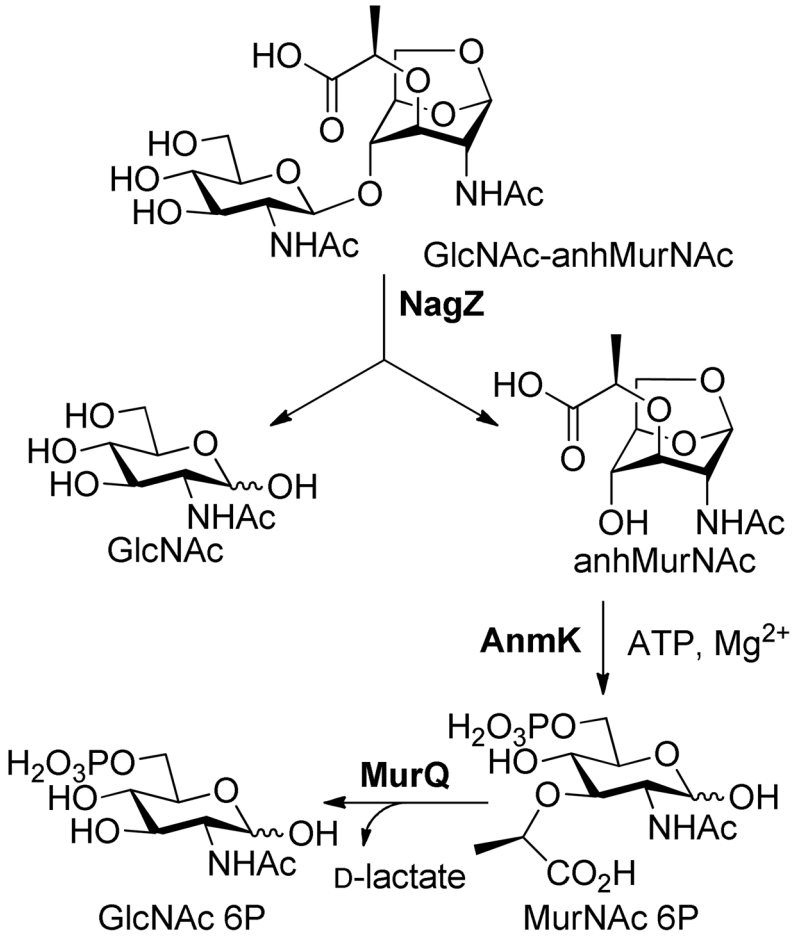

Figure 1.
Breakdown of the GlcNAc-anhMurNAc subunit via the peptidoglycan recycling pathway.

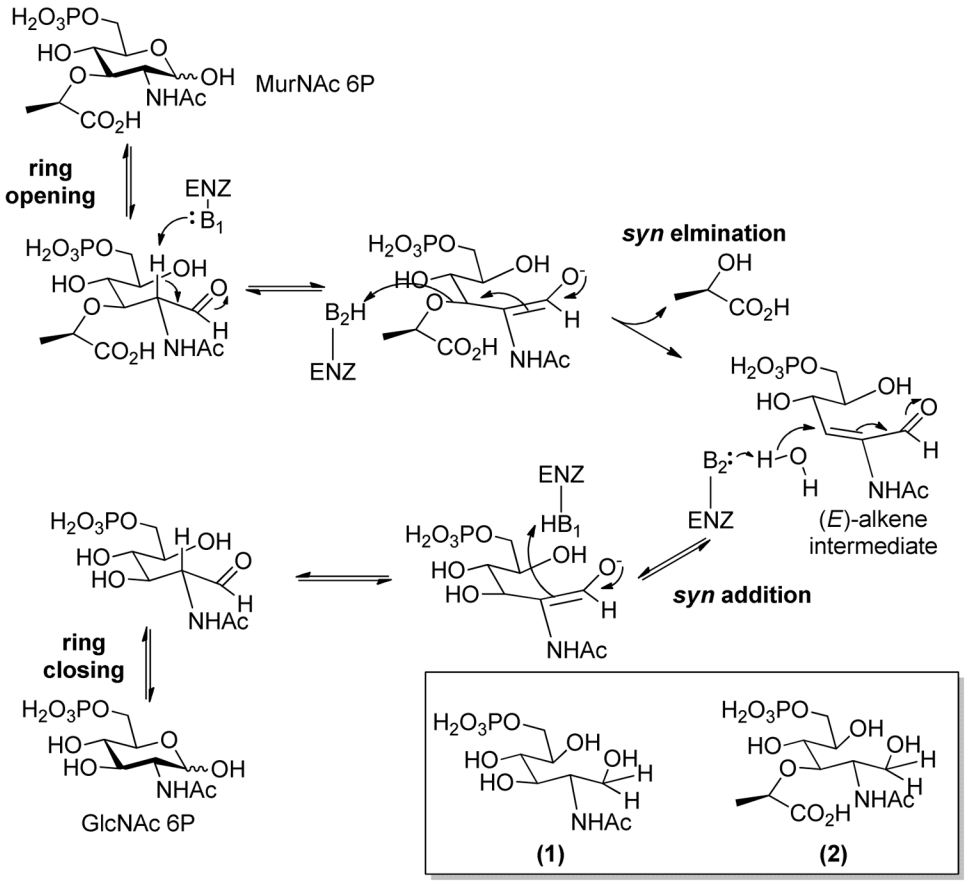

Figure 2.
Proposed mechanism of MurNAc 6P hydrolase catalysis and structures of GlcNAc 6P and MurNAc 6P open-chain analogs **1** and **2** (boxed).

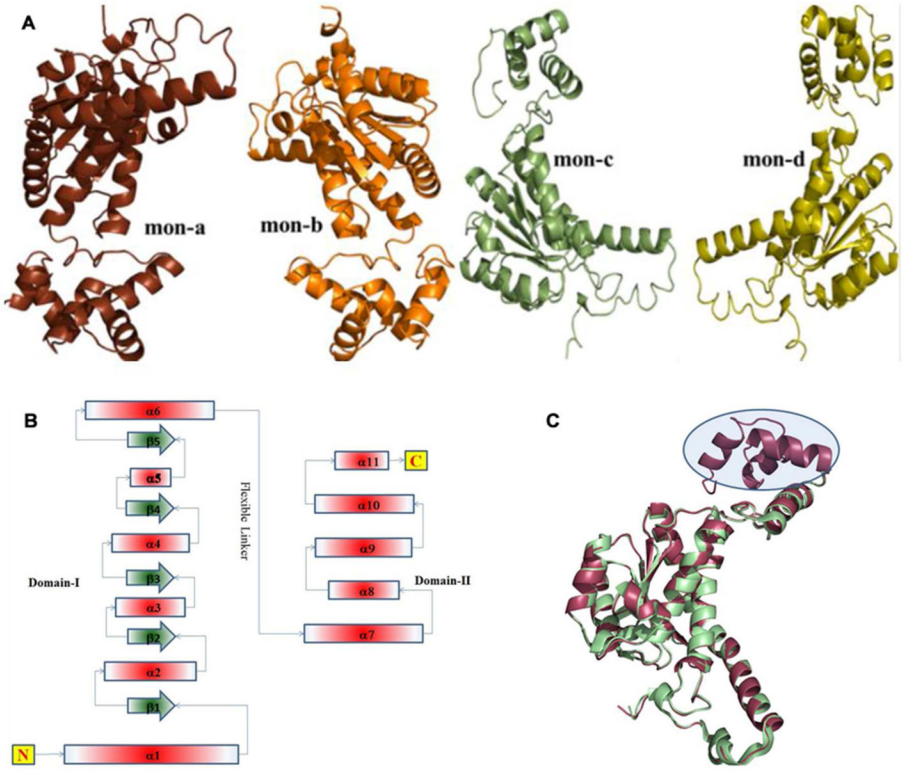

Figure 3.

The crystal structure of MurQ-HI. (A) Structure of the monomers A–D of MurQ-HI with bound compound **2**. (B) Secondary structure map of the MurQ-HI monomer. (C) Overlay of the MurQ-HI apo monomer (purple) with the previously solved monomer structure (green, PDB: 1NRI); the previously unsolved region is circled.

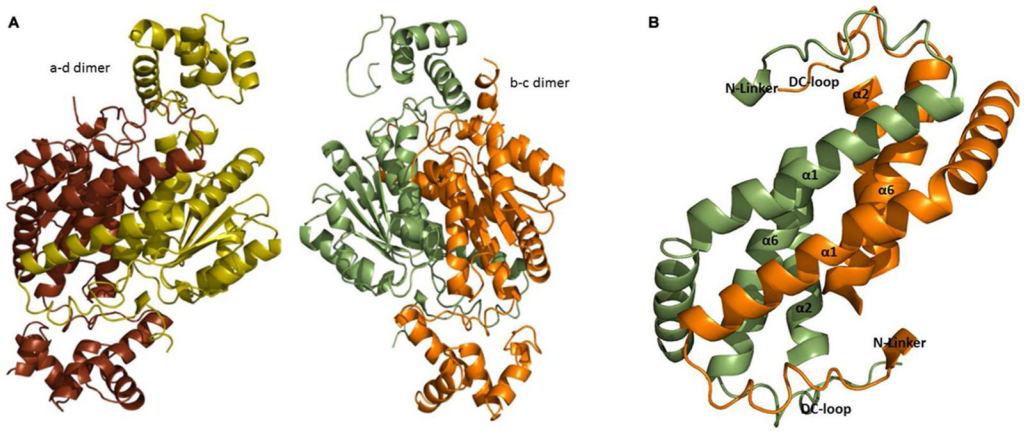

Figure 4.

(A) Structure of the MurQ-HI (with bound compound **2**) A–D and B–C dimers. (B) Dimer interface interactions between helices α1, α2, α6 and N-terminal and Domain-Connector (DC) loops.

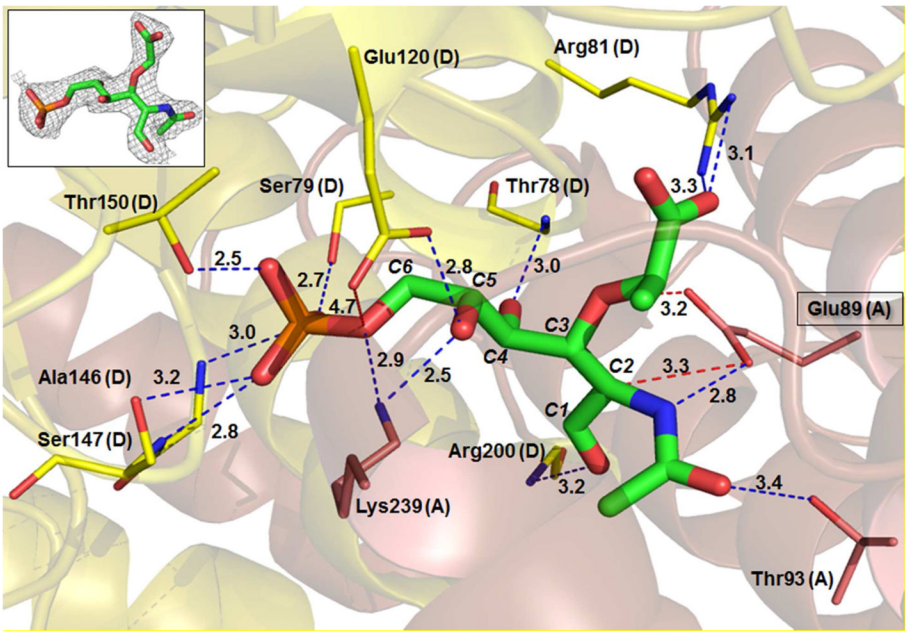

Figure 5.

Active site interactions in the MurQ-HI active site (Domains A/D) with compound **2** and electron density map of compound **2** (inset).

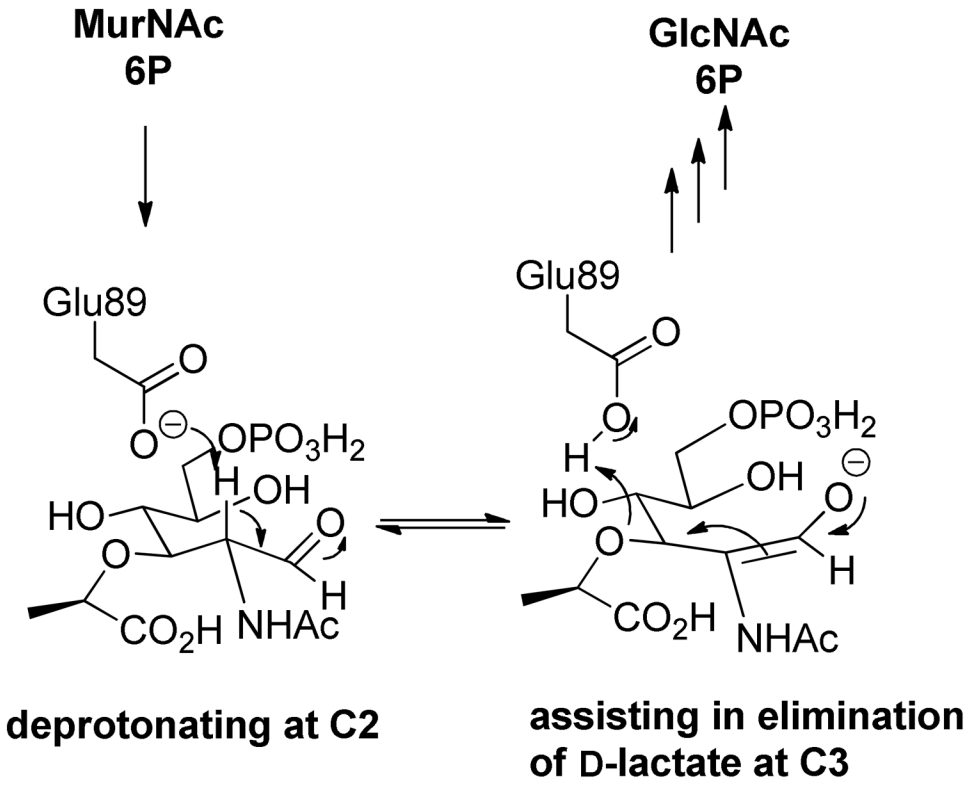

Figure 6.
Proposed dual role of Glu89 in MurQ catalysis.